Sequence-Responsive Unzipping DNA Cubes with Tunable Cellular Uptake Profiles

Supplementary Information

Katherine E. Bujold[1], Johans Fakhoury[1], Thomas G. W. Edwardson[1], Karina M. M. Carneiro[1], Joel Neves Briard[1], Antoine G. Godin[3], Lilian Amrein[2], Graham D. Hamblin[1], Lawrence C. Panasci[2,*], Paul W. Wiseman[1,3,*] and Hanadi F. Sleiman[1,*]

1. Department of Chemistry and Center for Self-Assembled Chemical Structures, McGill University, 801 Sherbrooke Street West, Québec H3A 0B8, Canada
2. Department of Oncology, Jewish General Hospital, 3755 Côte Sainte-Catherine Road, Québec H3T 1E2, Canada
3. Department of Physics, McGill University, 3600 University Street, Québec H3A 2T8, Canada

Contents

I. General

Reagents required for automated DNA synthesis, 1000 Å nucleoside-derivatized LCAA-CPG solid support (loading densities of 25-40 μmole/g) and Sephadex G-25 (super fine DNA grade) were purchased from BioAutomation. Dye-modified DNA strands were purchased from Integrated DNA Technologies with HPLC purification. Tris(hydroxymethyl)-aminomethane (Tris), magnesium chloride, acetic acid, boric acid, EDTA and urea required for buffer preparation as well as paraformaldehyde and StainsAll® were purchased from Aldrich. 1xTAMg buffer is composed of 45 mM Tris, 7.6 mM magnesium chloride and its pH is adjusted to 8.0 with acetic acid. 1xTBE buffer contains 90 mM Tris and boric acid and 1.1 mM EDTA. 40% acrylamide/bis-acrylamide 19:1 solution and HEPES were obtained from BioShop. Exonuclease VII (ExoVII, source: recombinant) and Mung Bean nuclease (MBN, source: mung bean sprouts) were purchased from BioLynx Incorporated. Dulbecco's Modified Eagle Medium (DMEM), RPMI 1640 medium, Opti-MEM medium, oligofectamine, Hoechst 33342 and ProLong Gold Antifade reagent were purchased from Invitrogen. Fetal bovine serum (FBS), 0.05% Trypsin-EDTA, phosphate-buffered saline (PBS), and sodium pyruvate were acquired from Wisent. The HeLa-GFP cells (that express a GFP-tagged histone protein specific to the nucleus) were a generous gift from Dr. Stephane Richard. The LNCaP clone FGC cells were purchased from ATCC.

II. Instrumentation

All standard DNA oligonucleotides were synthesized on solid support using a BioAutomation MerMade MM6 DNA synthesizer. Polyacrylamide gel electrophoresis (PAGE) was performed using 20 x 20 cm vertical Hoefer 600 electrophoresis units. A BioTek Synergy HT microplate reader and a NanoDrop Lite spectrophotometer was used to carry the UV-visible measurements required for DNA quantification. An Eppendorf Mastercycler® 96-well thermocycler was used to anneal the DNA samples. Calibration curves for concentrated cube solutions were obtained using a Cary 5000 UV-visible-NIR spectrophotometer. Melting temperature graphs were acquired on a Jasco J-810 spectrophotometer. FRET and dye

encapsulation experiments were conducted on a FluoroMax-2 fluorimeter. Dynamic light scattering experiments were conducted using a DynaPro instrument from Wyatt Technologies. The LC-MS data was obtained from a maXis impact instrument with an ESI source. Confocal microscopy images were obtained on a Quorum Wave FX-X1 Spinning Disc Confocal system equipped with the Volocity Imaging software. Flow cytometry data was acquired from a BD LSR Fortessa Analyzer with the FACSDiva software.

III. Oligonucleotides and Cube Design

The sequence design was performed so that the strands will assemble in the desired structure while minimizing undesired secondary interactions. At first, ten 10mer duplexes were defined and sequenced using a sequence generator (CANADA_2.0, available online). These were pooled with two additional asymmetric duplexes composed of 10mer duplexes with an 8-base single-stranded overhang that recognizes the *tpc-hpr* fusion gene to produce the final twelve vertices of the cube (see Figure 1c).

The sequences were then concatenated in six clips containing four of those duplexes according to the cube design. Two thymine bases were added between each 10mer duplex to provide flexibility for the cube to fold. This produced four 46mer strands and two 54mer strands (due to the 8-base overhang for *tpc-hpr* recognition) with the following pattern 5'-**A**-TT-**B**-TT-**C**-TT-**D**-3' where **A**, **B**, **C** and **D** are different 10mer duplexes.

Secondary interactions were then checked using the Oligo Analyzer 3.1 tool provided by Integrated DNA Technologies Inc. The threshold for secondary interactions between two different strands was set to 5 bases. An exception was made for the strand which contains the *tpc-hpr* sequence and its complement (Figure 1, purple strand). The *tpc-hpr* sequence in this case was slightly shifted around the fusion point to reduce this 10 base self-complementary region to a 7mer stem thereby allowing it to assemble in the desired structure.

The following table presents all the oligonucleotide sequences used in this edge article. Each of the strands forming the cube was assigned a number and a three-letter code referring to

the construct that will be made. For example, to go from the Unzipping Cube to the Blunt-Ended Cube, Unz-1 and Unz-5 need to be replaced with Dou-1 and Dou-5. The opened control is formed by replacing Unz-1 by CTL-1 which is not complementary to the other side of the cube and therefore prevents it from closing.

Table S1: Oligonucleotide sequences

Unzipping Cube (with *tpc-hpr* recognition domains)	
Name	**Sequence (5' to 3')**
Unz-1	AAAAGAAGAATTCAACTGTGAGTTGGACAGGCGTTTTTCCCACATATTTCTTCT
Unz-2	ACGCCTGTCCTTTTGCGACCTTTTTGTGTGCCGTTTCAATACACGC
Unz-3	CTCACAGTTGTTATGAAGTACATTATCGCTCCATTTAAGGTCGCAA
Unz-4	ATGGAGCGATTTGCACCACTTATTCCCATGACTGTTACGGCACACA
Unz-5	CCACATATTTCTTCTTTTTTCGTTCCGGTTTTTAAGTGGTGCTTTGTACTTCAT
Unz-6	AACCGGAACGTTTATGTGGGAATTGCGTGTATTGTTCAGTCATGGG
Unzipping Cube Markers	
Name	**Sequence (5' to 3')**
tpc/hpr-21	AAAAGAAGAAATATGTGGGAA
RNA-21	AAAAGAAGAAAUAUGUGGGAA
tpc-21	CTATCAGAAGAAAAAGAAGAA
hpr-21	ATATGTGGGAAGCCCAAGAAT
Opened Cube and Control Cube with fully randomized sequences	
Name	**Sequence (5' to 3')**
CTL-1	GACCCTTCGATTCAACTGTGAGTTGGACAGGCGTTTTAAAGCCCTAGTTCAGAG
CTL-5	ACCTATTCTCGAAGGGTCTTCGTTCCGGTTTTTAAGTGGTGCTTTGTACTTCAT
CTL-6	AACCGGAACGTTTAGGGCTTTATTGCGTGTATTGTTCAGTCATGGG

Markers for Opened Cube and Control Cube with fully randomized sequences	
Name	**Sequence (5' to 3')**
Fla-2	GACCCTTCGAGAATAGGTATC
Fla-3	CTGCTCTGAACTAGGGCTTTA
Blunt-ended Cube	
Name	**Sequence (5' to 3')**
Dou-1	AAAAGAAGAATTCAACTGTGAGTTGGACAGGCGTTTTTCCCACATA
Dou-5	TTCTTCTTTTTTCGTTCCGGTTTTTAAGTGGTGCTTTGTACTTCAT
Fluorescent strands for FRET	
Name	**Sequence (5' to 3')**
Cy5-2	Cy5-ACGCCTGTCCTTTTGCGACCTTTTTGTGTGCCGTTTCAATACACGC
Cy3-6	AACCGGAACGTTTATGTGGGAAT-Cy3-TGCGTGTATTGTTCAGTCATGGG

DNA synthesis and purification was performed following standard protocols[1] at the 1 μmole scale. Briefly, deprotection was carried according to the manufacturer's specifications in 1:1 ammonium hydroxide: methylamine solutions for 30 minutes at room temperature followed by 30 minutes at 60^{o}C if (strands of 50 bases or less) or for 90 minutes at room temperature followed by 60 minutes at 60^{o}C (strand is 50 bases and more). The crude product was dried and resuspended in 1:1 water: urea solutions to be loaded on 15-19% polyacrylamide/8M urea gels (PAGE) with 1xTBE running buffer. The gels were run for 30 minutes at 250 V, followed by 60 minutes at 500 V using a constant current of 30 mA per gel. The gels were then imaged on a fluorescent TLC plate under a UV lamp (254 nm) and quickly excised. The bands were crushed and soaked in autoclaved Milli-Q water at 60^{o}C overnight to extract the DNA from the gel. Following this, the samples were dried until they reached a volume of 1 ml. They were then desalted using size exclusion chromatography columns (Sephadex G-25) and quantified by UV-visible spectroscopy in triplicates using the maximal DNA absorption peak at 260 nm. Concentrations in μmoles were calculated from the extinction coefficients obtained from the Oligo Analyzer 3.1 tool (Integrated DNA Technologies Inc) for the given sequence.

The DNA strands modified with **C_{12} D-DNA** or **HEG D-DNA** were synthesized using the procedure described by Edwardson *et al.*[2] Briefly, strands Unz-1 to Unz-4 and Unz-6 were

synthesized using standard automated protocols with an additional spacer consisting of two thymines added on the 5' end. Two symmetrical branches (ChemGenes, cat.# CLP-5215) were then added followed by DMT-dodecane-diol phosphoramidite (ChemGenes, cat.# CLP-1114) for the **C_{12} D-DNA** or DMT-hexaethyloxy glycol-phosphoramidite (ChemGenes cat.# CLP-9765) for the **HEG D-DNA** strands. These reagents were dissolved in anhydrous dichloromethane (DMT-dodecane-diol phosphoramidite) or acetonitrile (symmetrical branch, DMT-hexaethyloxy glycol phosphoramidite) to a final concentration of 0.1M and added on the DNA synthesizer. Extended coupling times (5 to 15 minutes) were used to allow the reactions to go to completion.

Alternatively, to maximize the yields, these reactions were performed in a glove box under a nitrogen atmosphere using anhydrous dichloromethane (DMT-dodecane-diol phosphoramidite) or acetonitrile (symmetrical branch, DMT-hexaethyloxy glycol phosphoramidite) to dissolve the reagents to a final concentration of 0.1 M. These were added to the columns along with an equal volume of ethylthiotetrazole (0.1M in acetonitrile) and allowed to couple for 15 minutes with manual mixing. After the couplings were completed, the columns were returned to the synthesizer for the capping, oxidization and deblocking steps. Coupling efficiencies were monitored from the removal of the DMT group which has a strong absorbance peak at 498 nm.

The structure of the **C_{12}** and **HEG D-DNA** strands was confirmed by LC-MS using an ESI source. The samples were first purified using denaturing PAGE gels (15%) followed by reverse phase HPLC using the procedure described by Edwardson *et al.*[2] prior to the run. Results are summarized in table S2.

Table S2: Calculated and experimental masses obtained from LC-MS for the D-DNA modified strands.

Name	Calculated mass (g/mol)	Experimental mass (g/mol)
Unz-1 TT C_{12} D-DNA	18736.6	18735.6
Unz-2 TT C_{12} D-DNA	16127.9	16127.1
Unz-3 TT C_{12} D-DNA	16226.0	16225.2
Unz-4 TT C_{12} D-DNA	16197.0	16196.2
Unz-6 TT C_{12} D-DNA	16434.1	16433.2
Unz-1 TT HEG D-DNA	19056.6	19056.0
Unz-2 TT HEG D-DNA	16447.9	16447.2
Unz-3 TT HEG D-DNA	16546.0	16545.0
Unz-4 TT HEG D-DNA	16517.0	16516.5
Unz-6 TT HEG D-DNA	16754.1	16753.3

IV. Cube assembly and Opening

Cube assembly and opening assays by PAGE were conducted under native conditions to preserve DNA interactions. Samples for native PAGE analysis were prepared in 1xTAMg with 0.01 OD of DNA (0.27 µM). For this purpose, stock solutions of 0.002 OD/µl in 1xTAMg were prepared for each DNA strand using the extinction coefficient of Unz-1 for normalization to account for the different optical properties of strands with different lengths and keep equal molar ratios of each strand. Sample volumes were then adjusted to 12 µl with 1xTAMg and the samples were thermocycled from 95°C to 4°C in 5.5 hours. Glycerine (2 µl) was added before loading for a final volume of 14 µl. Samples were run on 7 or 8% native gels for 150 minutes at 250 V and 50 mA with 1xTAMg running buffer. Gels were subsequently stained in StainsAll® or GelRed™ and scanned.

All the strands involved in the cube formation were combined in one pot before thermocycling. For cube opening assays, two equivalents of the appropriate synthetic marker were added after thermocycling at room temperature 5 minutes prior to loading on gel (with the exception of the fully asymmetric cube where two different markers were used instead). Cube opening studies also revealed that the "double cube" side product opens following the same mechanism as the cube since the band disappears when the marker is added.

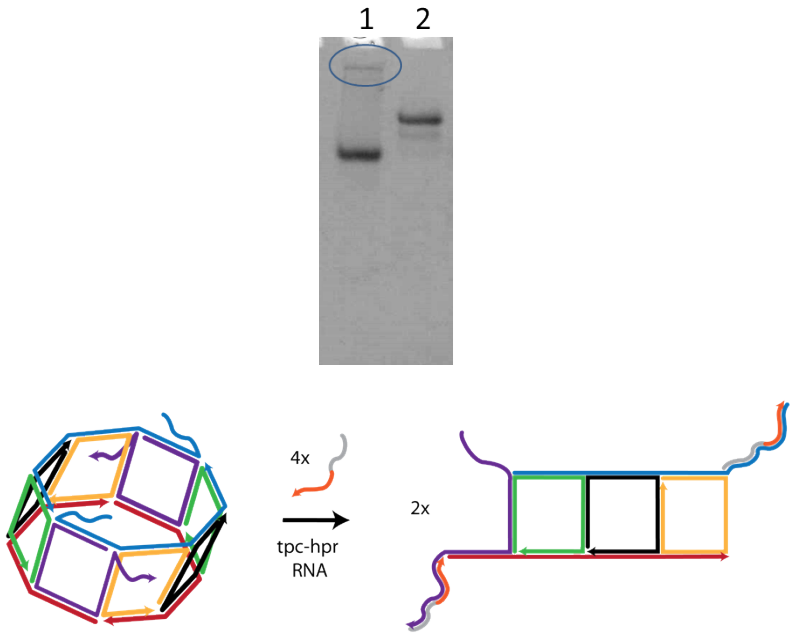

Figure S1: "Double cube" disappearance after *tpc-hpr* synthetic marker addition. The circled band in lane 1 corresponds to the "double cube" side product. The band below is the cube. After addition of the *tpc-hpr* marker (lane 2) the "double cube" band disappears and there is only one major product. This suggests that the "double cube" side product opens up to form two opened cube structures (right).

Further characterization of the cube was carried using Exonuclease VII (ExoVII) and Mung Bean nuclease (MBN) exonucleases. Cubes samples were prepared and assembled at room temperature to see which products in the crude mixture could correspond to the cube (closed and cyclic). ExoVII was used to verify if the structure was fully closed since it exhibits a high specificity towards single stranded DNA and has both 5' to 3' and 3' to 5' exonuclease activities. Native PAGE samples of the cube and its opened version were incubated with 5 units of ExoVII for 2 hours at 15°C. The samples were then loaded and run on 8% native PAGE gels. Results indicate that the cube and the octagonal prism are both cyclic and closed as opposite to the

opened cube which gets degraded by the enzyme. Mung Bean nuclease was used to verify the double stranded character of the cube since this endonuclease will degrade specifically single-stranded extensions from DNA or RNA. For this assay, native PAGE samples were incubated with 2.5 units of the enzyme and incubated for 1 hour at 30°C. The samples were then also loaded and run on 8% native PAGE gels. From this assay, it appears that the blunt-ended cube and the cube are both resistant to the enzyme thus highlighting their double stranded character.

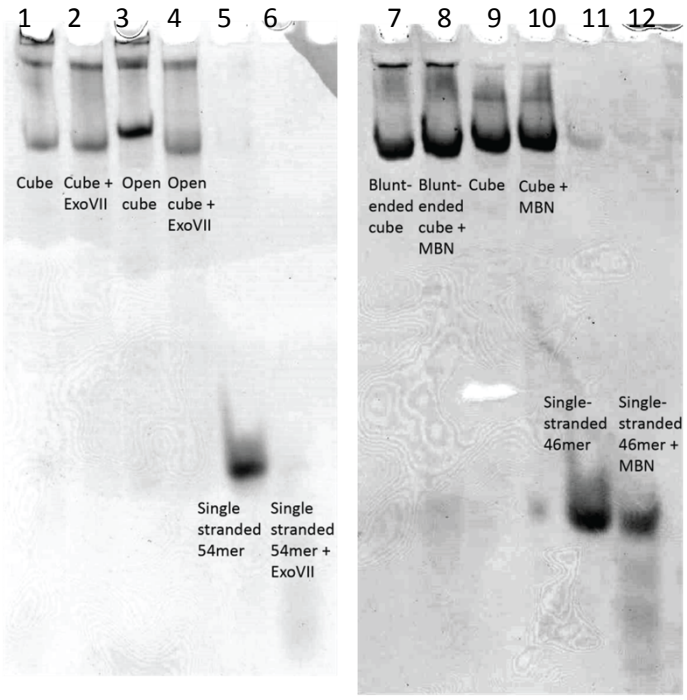

Figure S2: Exonuclease VII and Mung Bean nuclease assays on the cube assembled at room temperature. Lane 1 is the cube control while lane 2 is the cube with ExoVII which has not been degraded. Lane 3 shows the opened cube which is degraded in lane 4. The same thing is observed in lanes 5 and 6 where a single stranded 54mer is degraded by the enzyme. In lanes 7 and 8, the blunt-ended cube is put in presence of Mung Bean nuclease and resists the treatment. The same is observed in lanes 9 and 10 where the cube is not degraded by the enzyme. The single stranded 46mer control in lanes 11 and 12 gets degraded by the enzyme.

The assembly of the $\mathbf{C_{12}}$ and **HEG** cubes was verified using 7% native PAGE gels similarly to what was done on Figure 1b) and following the protocol described at the top of section IV. Briefly, each of the strands composing these cubes was added sequentially in order to form a larger structure. The clean assembly of the product was confirmed by the lower mobility

of the bands obtained after each addition. Cube opening was also verified using an excess of the synthetic *tpc-hpr* marker.

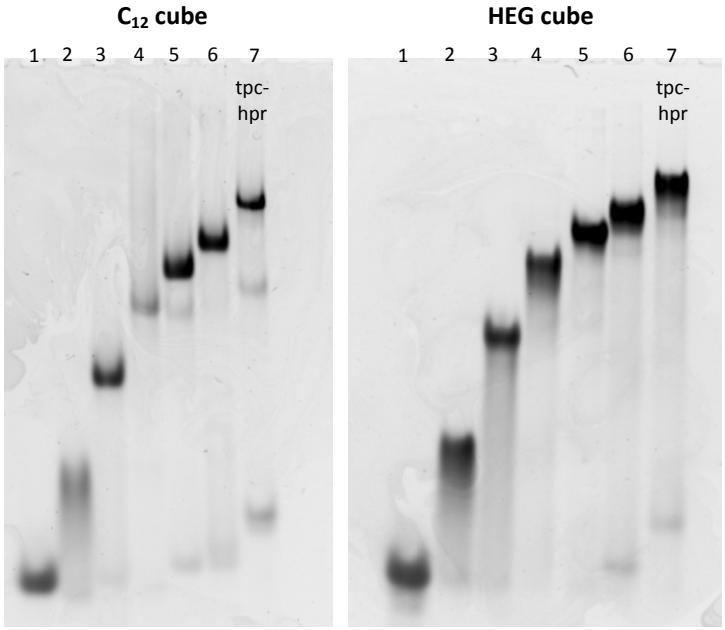

Figure S3: Assembly and opening of the C_{12} (left) and HEG (right) cubes. Lanes 1 through 6 show the stepwise assembly of the cube with lane 6 being the fully assembled product. In lane 7, an excess of the *tpc-hpr* marker was added to verify that the opening of the cube was unhindered by the D-DNA chains.

A preliminary appreciation of the size of the D-DNA modified cubes compared to the unmodified cubes was obtained using PAGE. An 8% native gel was run with the unmodified cube, the **C_{12}** cube and the **HEG** cube side by side (Figure S4). It appears that the **HEG** cube forms the largest structure, likely due to the **HEG D-DNA** chains being hydrophilic and extending outwards. The **C_{12}** cube appears smaller than the **HEG** cube but bigger than the unmodified cube likely due to its more hydrophobic chains collapsing on the surface of the cube, thus providing an exterior coating to the DNA structure.

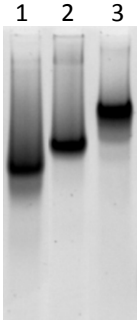

Figure S4: Gel mobility comparison for the unmodified cube, C_{12} cube and HEG cube. Native PAGE gel (7%), lane 1 shows the unmodified cube, lane 2 the C_{12} cube and lane 3 the HEG cube. The three construct are in increasing size order as reflected from band mobility analysis.

V. Fluorescence Experiments *In Vitro*

For these assays, FRET dyes were placed on the cube so that they are in close proximity when the cube is closed and separated when the cube is opened. The Unz-2 strand was replaced with Cy5-2 which contains a Cy5 dye (acceptor) at the 5' position and Unz-6 was replaced with Cy3-6 which has a Cy3 dye (donor) positioned in the middle of the strand. This dye placement, on the bottom corner of the cube, was selected because it did not hinder cube assembly and opening by PAGE and allowed for a good separation between the dyes when the cube is opened (Figure S5).

Figure S5: Cy3 and Cy5 dually-labeled cube and blunt-ended cube. On the left is the cube dually-labeled with Cy3 and Cy5 while the dually-labeled blunt-ended cube is on the right. The dyes do not alter cube assembly.

FRET experiments were carried with samples containing 12 picomoles of cubes modified with Cy3, Cy5 or both. These were pre-assembled using a 5.5-hour 95^{o}C to 4^{o}C thermal anneal

at a concentration of 0.22 µM in 1xTAMg. The samples were diluted to a final volume of 500 µl with 1xTAMg (final concentration of 24 nM). Concentrated synthetic markers were added in 2x excess 5 minutes before measuring the fluorescence intensity of the dyes when required.

A wavelength of excitation of 550 nm was used to excite the Cy3. If Cy5 was in close proximity, a fluorescence peak around 670 nm would appear corresponding to Cy5 emission as a result of the energy transfer between the two dyes. These experiments were done in triplicates. The efficiency of transfer between the two dyes for each of the different constructs was calculated using the following equation:

$$E_{FRET} = 1 - F_{DA}/F_D$$

where E_{FRET} is the efficiency of transfer between the two dyes, F_{DA} is the fluorescence intensity of the donor in the presence of the acceptor and F_D is the fluorescence intensity of the donor alone. As expected, all closed structures exhibited high efficiencies of transfer and all opened cubes displayed a lower E_{FRET}. The following figure summarizes the results obtained with different constructs.

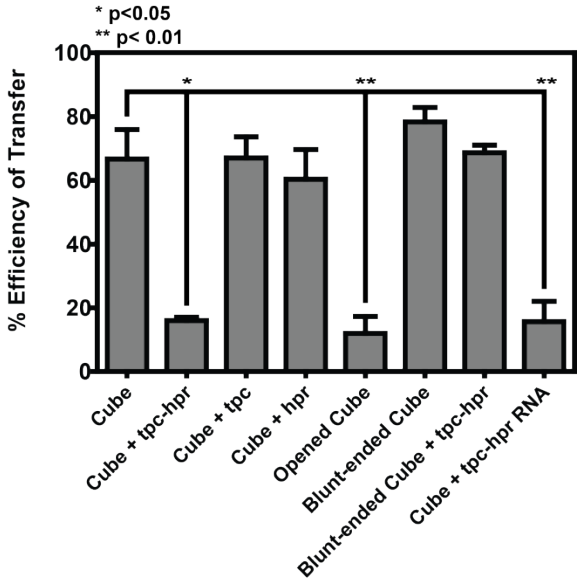

Figure S6: Efficiency of transfer for different cube constructs. The efficiency of transfer from Cy3 and Cy5 was evaluated for different cube constructs. The efficiency of transfer for closed constructs (cube, cube + *tpc*, cube + *hpr*, blunt-ended cube and blunt-ended cube + *tpc-hpr*) was found to oscillate between 60% and 80% suggesting that the dyes are in close proximity. The E_{FRET} for opened constructs (cube + *tpc-hpr*, opened cube and cube + *tpc-hpr* RNA) was found to be below 20% suggesting that the dyes are separated by a significant distance.

The fluorescent dye encapsulation experiments were based on the procedure elaborated by Edwardson *et al.*[2] Briefly, the unmodified cube and the **C_{12}** cube (250 nM, 200 µl) were assembled in 1xTAMg buffer using a 5.5 hour thermal anneal from 95°C to 4°C. Nile Red or 1,6-diphenyl-1,3,5-hexatriene (DPH) were then added to a final concentration of 5 µM from concentrated stocks solutions at 1 mM in acetone and the samples were left to incubate at room temperature in the dark for 24 hours. The samples were then centrifuged twice (15 000 x g, 20 min) using Amicon Ultra 10K centrifugal filters to remove the free dye in solution. The remaining cubes were denatured in 3:1 acetone:buffer solutions and the fluorescence of the resulting samples was measured. For Nile Red, the excitation wavelength was 535 nm with a slit width of 5 nm and the emission was collected from 550 to 750 nm. For DPH, the excitation wavelength was 350 nm with a slit width of 5 nm and the emission was collected from 570 to 770 nm.

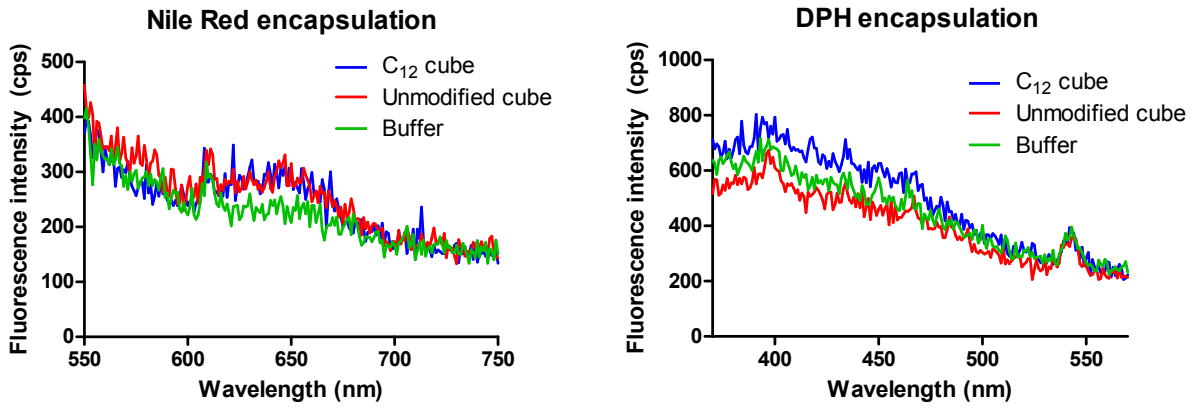

Figure S7: Nile Red (left) and DPH (right) encapsulation in the unmodified cube and the C_{12} cube. The encapsulation of either dye is not significant since all three curves (C_{12} cube, unmodified cube and buffer) are overlaid. This suggests that the C_{12} D-DNA modified cube does not form a significant lipid pocket for the dyes to fluoresce.

The results from the encapsulation experiment showed that there was no significant encapsulation of either dye, thereby suggesting that no significant lipid pocket was created inside the cube from the addition of the **C_{12} D-DNA** chains. They also support the hypothesis that the **C_{12} D-DNA** chains are not forming a micelle inside the DNA cube but are instead likely coating the exterior of the cube.

VI. Melting Temperature

The melting temperature of the cube was evaluated to verify its stability in biological conditions. Melting was performed on pre-assembled cube solutions in 1xPBS (1 μM in 150 μl) on a spectropolarimeter and absorption at 260 nm was monitored. 1xTAMg buffer was not used as the solvent because magnesium tightens DNA interactions, thus increasing the melting temperature of the construct. This is not representative of cellular environments which have a much lower Mg^{2+} concentration, thus justifying the use of 1xPBS. For this purpose, seven cube samples at a concentration of 2.5 μM (100 μl) were prepared. These were then concentrated using microcon centrifugal filtration columns (10K MWCO). The cubes were centrifuged twice for 15 minutes at room temperature. The concentration of the resulting samples was determined by UV-visible spectroscopy from a constructed calibration curve. For the melting, the temperature was raised from 25°C to 75°C at a rate of 1°C per minute. The melting temperature of the cube was found to be 45°C which is amply sufficient for biological assays.

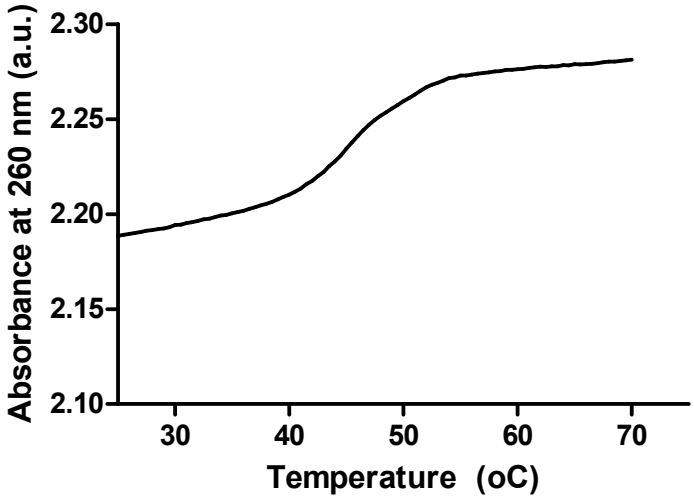

Figure S8: Melting temperature of the cube in 1xPBS. From the melting curve, the melting temperature of the cube was found to be 45°C which is well above the requirement for biological applications.

VII. Serum Stability Assays

The serum stability assays were conducted for 48 hours according to the procedure developed by Conway *et al.*[3] Briefly, concentrated samples of the cube and the blunt-ended cube were prepared as described in the melting temperature section. This was done to once again reduce the Mg^{2+} present in the assay as it activates some the enzymes in fetal bovine serum; as a result, the half-lives of the constructs under study appear to be reduced which is not representative of their actual behaviour in biological conditions. For this purpose, the assay was run in DMEM medium instead of 1xTAMg. The assay volume was set to be 150 µl (V_{assay}) to get at least 10 aliquots of 10 µl each (at 0, 1, 2, 3, 4, 6, 8, 12, 24 and 48 hours) for each sample. The assay concentration was set at 0.4 uM ([assay]). From the concentrations ([construct]) obtained from the calibration curves (44.67 µM for the cube and 43.42 µM for the blunt-ended cube), the volume of each construct necessary for the assay was computed as follows using the dilution equation:

$$V_{construct} = \frac{[assay] * V_{assay}}{[construct]}$$

where $V_{construct}$ is the volume of cube or blunt-ended cube required for the assay. A single-stranded 46mer was used as a control and was prepared using the same method except that it did not need to be concentrated prior to the assay. 1xTAMg was added up to 2 ul to keep the concentration of Mg^{2+} in each sample constant. DMEM (133 ul) and FBS in 10% v/v (15 ul) were added to start the assay. The FBS assay was done in triplicates. Aliquots were stored in the freezer at -20°C in 5 ul glycerine to inactivate the enzymes after each time point. At the end of the assay, the samples were loaded on 8% native polyacrylamide gels and run for 150 minutes at 250 V and 50 mA. These were then stained overnight in StainsAll® before analysis. Table S3 summarizes the assay conditions and Figure S9 shows sample gels obtained from this assay.

Table S3: FBS assay conditions for the cube, blunt-ended cube and single stranded 46mer.

Construct	Concentration (µM)	Assay volume (µl)	Assay concentration (µM)	Construct (µl)	1xTAMg (µl)	DMEM (µl)	FBS (µl)	Picomoles per aliquot
Cube	44.67	150	0.4	1.34	0.66	133	15	4
BE Cube	43.42	150	0.4	1.38	0.62	133	15	4
46mer	109.77	150	0.4	0.55	1.45	133	15	4

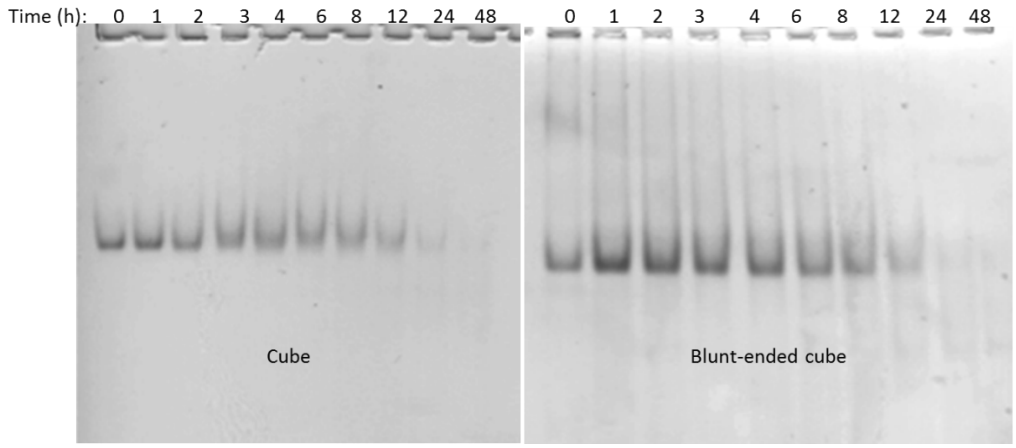

Figure S9: Sample gels obtained for the cube and blunt-ended cube. Aliquots of the cube and blunt-ended cube in 10% FBS/DMEM solution were taken at different time points. The band density was evaluated with ImageJ to extract information about the decay of the cube over time.

The gels were analysed using ImageJ to evaluate the band density over time. The bands were selected from the zero time point using the Analyze/Gels tool. The area under the density peaks was measured for each time point and plotted versus time. The data was then fitted in GraphPad using the "Nonlinear regression" tool with "One phase decay" as the chosen parameter. The zero time point was excluded from the analysis for all samples. All R^2 values for the fits were above 0.8 as shown below.

Table S4: R^2 values for the one phase decay fit

Construct	R^2
Cube	0.9463
Blunt-ended cube	0.8842
Single-stranded 46mer	0.8287

The second FBS assay was run using the same procedure using the unmodified cube, the $\mathbf{C_{12}}$ cube, the **HEG** cube and a single-stranded 46mer (same as above) as samples using 7% native polyacrylamide gels (Figure S10). The assay was run for 72 hours to match the incubation time of the FACS procedure using the same ten time points as above with an additional one at 72 hours for a total of eleven aliquots per sample. In order to obtain higher quality scans, the procedure was slightly altered. First, Stainsall® was replaced by a more sensitive stain, GelRed®

and to account for this the volume of the aliquots was reduced by half. Second, the volume of 1xTAMg was increased from 2 µl to 5 µl in each sample to account for the lower concentration of each cube construct (Table S5). Finally, ImageLab was used as software instead of ImageJ in the first part of the analysis. Briefly, the analysis was carried by manually defining the lanes and bands in the gel which corresponded to the construct of interest using the Lanes and Bands tool. Then, the first band (zero time point) was set a reference for band density calculations using Quantity tools. The data obtained from each band was then plotted and fitted to a one phase decay using GraphPad. R^2 values for these fits are summarized in Table S6.

Table S5: FBS assay conditions for the unmodified cube, C_{12} cube, HEG cube and 46mer.

Construct	Concentration (uM)	Assay volume (ul)	Assay concentration (uM)	Construct (ul)	1xTAMg (ul)	DMEM (ul)	FBS (ul)	Picomoles per aliquot
Cube	25.41	150	0.4	2.36	2.64	130	15	2
C_{12}	13.92	150	0.4	4.31	0.69	130	15	2
HEG	19.91	150	0.4	3.01	1.99	130	15	2
46mer	99.72	150	0.4	0.60	0.89	130	15	2

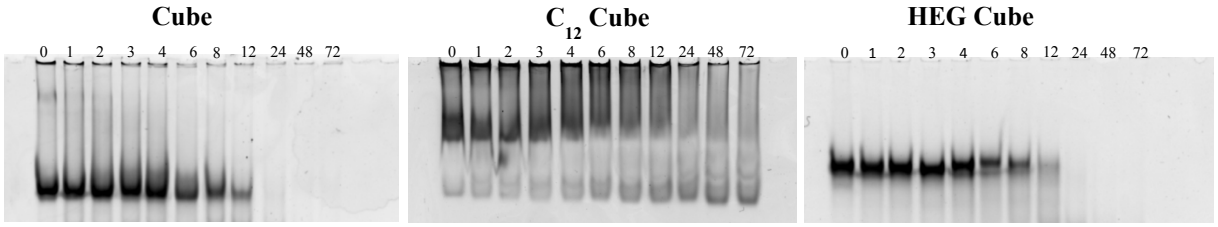

Figure S10: Sample gels obtained for the cube, the C_{12} cube and the HEG cube. Aliquots of the cube and blunt-ended cube in 10% FBS/DMEM solution were taken at different time points. The band density was evaluated with ImageLab to extract information about the decay of these constructs over time.

Table S6: R^2 values for the one phase decay fit

Construct	**R^2**
Cube	0.8624
HEG cube	0.9028
46mer	0.8223

VIII. Dynamic Light Scattering

Dynamic light scattering (DLS) experiments were carried at 25°C to evaluate the size of different cube constructs with respect to each other (unmodified cube, **C_{12}** cube and **HEG** cube). 1xTAMg buffer was used as a control. For this experiment, the cube solutions under study were concentrated to 5-10 μM using Amicon Ultra 10K centrifugal filters and filtered using 0.45 μm Nylon syringe filters. Hydrodynamic radius measurements were repeated a minimum of five times for each sample. The hydrodynamic radius, %polydispersity, %mass and number of repeats (n) are reported in the table below and the error is derived from the standard deviation of multiple measurements. The concentrated cube samples were then run on 7% native gel to verify that they are main species in solution. Significant aggregation was observed for the **C_{12}** cube and unmodified cube after concentrating the samples to 20 μM. As a result, the DLS experiments were performed at lower concentration of 10 μM where aggregation is greatly reduced. No aggregation was observed in the case of the **HEG** cube (5 μM samples).

Table S7: Hydrodynamic radius and % polydispersity of different cube constructs from dynamic light scattering.

Construct	Hydrodynamic radius (nm)	% Polydispersity	%Mass	n
Unmodified cube	4.7 ± 0.3	9.7 ± 6.8	90.5 ± 3.4	12
C_{12} cube	5.6 ± 0.2	13.7 ± 4.8	97.7 ± 0.6	10
HEG cube	6.1 ± 0.1	20.5 ± 4.6	99.8 ± 0.1	5

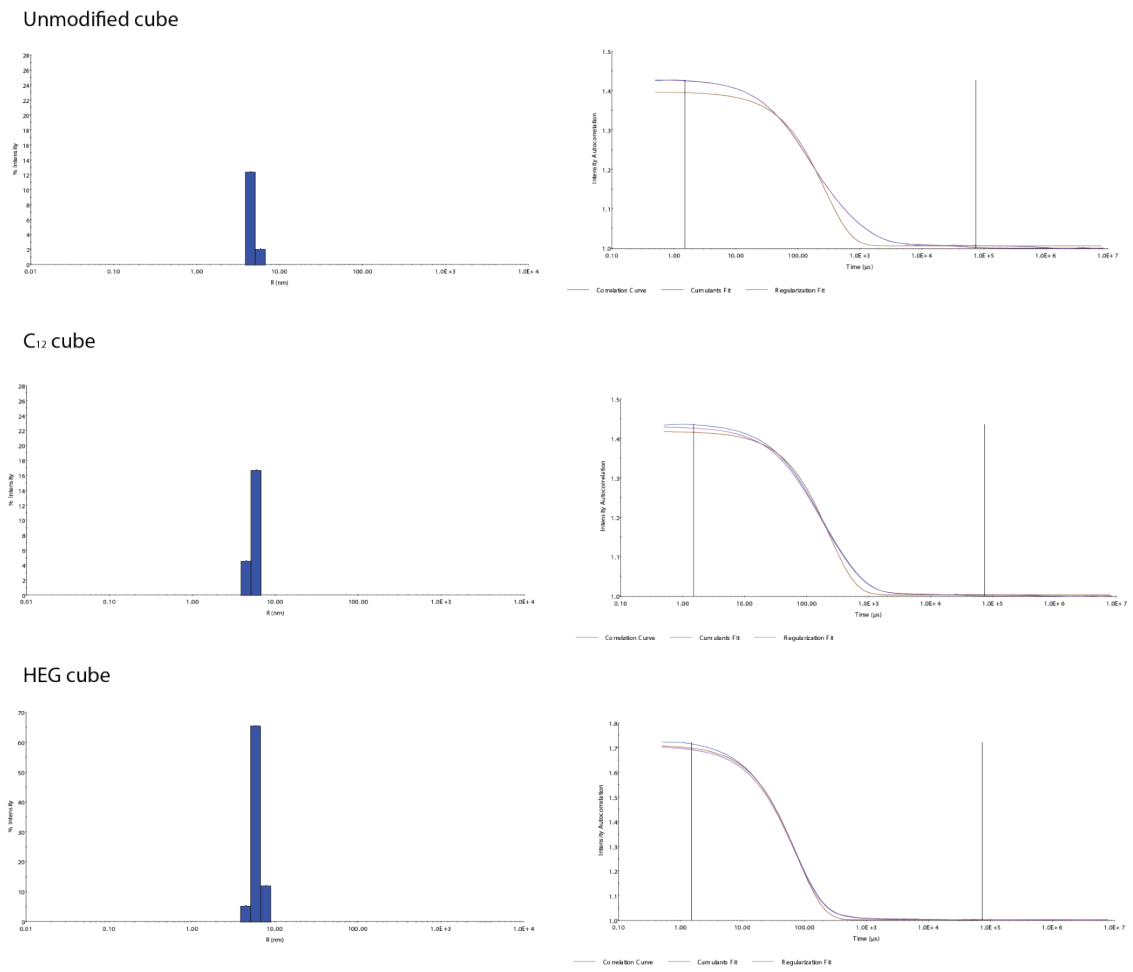

Figure S11: Dynamic light scattering experiment on different cube constructs. DLS regularization distributions histograms and correlation functions are shown for the unmodified cube, the C_{12} cube and the HEG cube (10 μM solutions). All constructs display good correlations. Residual buffer peaks were removed for clarity.

IX. Cellular Uptake Experiments

a) Cell Propagation

HeLa-GFP cells were propagated in DMEM medium supplemented with 10% FBS and antibiotic/antimycotic. Cells were passaged every 2-3 days at a ratio of 1:4. Cells were incubated at 37°C with 5% CO_2.

LNCaP clone FGC cells were propagated in RPMI 1640 medium supplemented with 10% FBS, 10 mM HEPES, 1 mM sodium pyruvate and antibiotic/antimycotic. Cells were passaged every 3-4 days at a ratio of 1:4. Cells were incubated at 37^{o}C with 5% CO_2.

Chronic Lymphocytic Leukemia (CLL) cells were obtained from patients with a diagnosis of B-CLL followed at the Jewish General Hospital of Montreal who enrolled in the study after informed consent. CLL cells are suspension cells and non-adherent. As a result, they have a different morphology than adherent monolayer cells. Lymphocytes were isolated from the peripheral blood using Ficoll-Hypaque (Pharmacia, Uppsala, Sweden) as described[4]. Briefly, Heparinized blood obtained from patients with CLL was layered onto Ficoll-Hypaque reagent and centrifuged for 40 min at 500 x g at room temperature. The interface was removed, washed twice, and suspended in RPMI media supplemented with 10% heat inactivated FBS[5]. The isolated lymphocyte population was >95% malignant B-lymphocytes. The B-CLL lymphocytes were maintained in DMEM media.

Since the CLL cell samples were collected from different patients in limited amounts, assays could not be run in triplicates. Instead, the results shown are representative examples from one patient.

b) Confocal microscopy

For confocal microscopy, typically cells were seeded at a concentration of 50 cells/µl (100 000 cells in 2 ml) in 6-well plates which contained ethanol-washed coverslips one day prior to the sample incubation. The medium was then replaced in each well with medium without serum (1 ml) and cube samples were added (250 picomoles in 100-200 µl, 1.25-2.5 µM). The cells were incubated for 4 hours at 37^{o}C with 5% CO_2 after which 10% v/v FBS was added (120 µl). The cells were incubated for another 2 or 22 hours (total of 6 or 24 hours of incubation with the DNA samples). Cells were then washed three times with PBS (1 ml) and fixed with a 4% paraformaldehyde/PBS solution (1 ml) for 30 minutes in the dark at 4^{o}C. The cells were next thoroughly washed three times with PBS (1 ml).

To stain the nuclei of the LNCaP cells, Hoechst 33342 was added to the last rinse at a 10 μg/ml concentration and mixed gently in the dark for 15 minutes at room temperature. The cells were rinsed three times with cold PBS following the staining.

The coverslips were then mounted on microscope slides with 1 drop of ProLong gold mounting medium and sealed. The slides were checked under the microscope and stored at 4°C until visualization. The following figures provide representative examples of what was observed in HeLa, LNCaP and CLL cells.

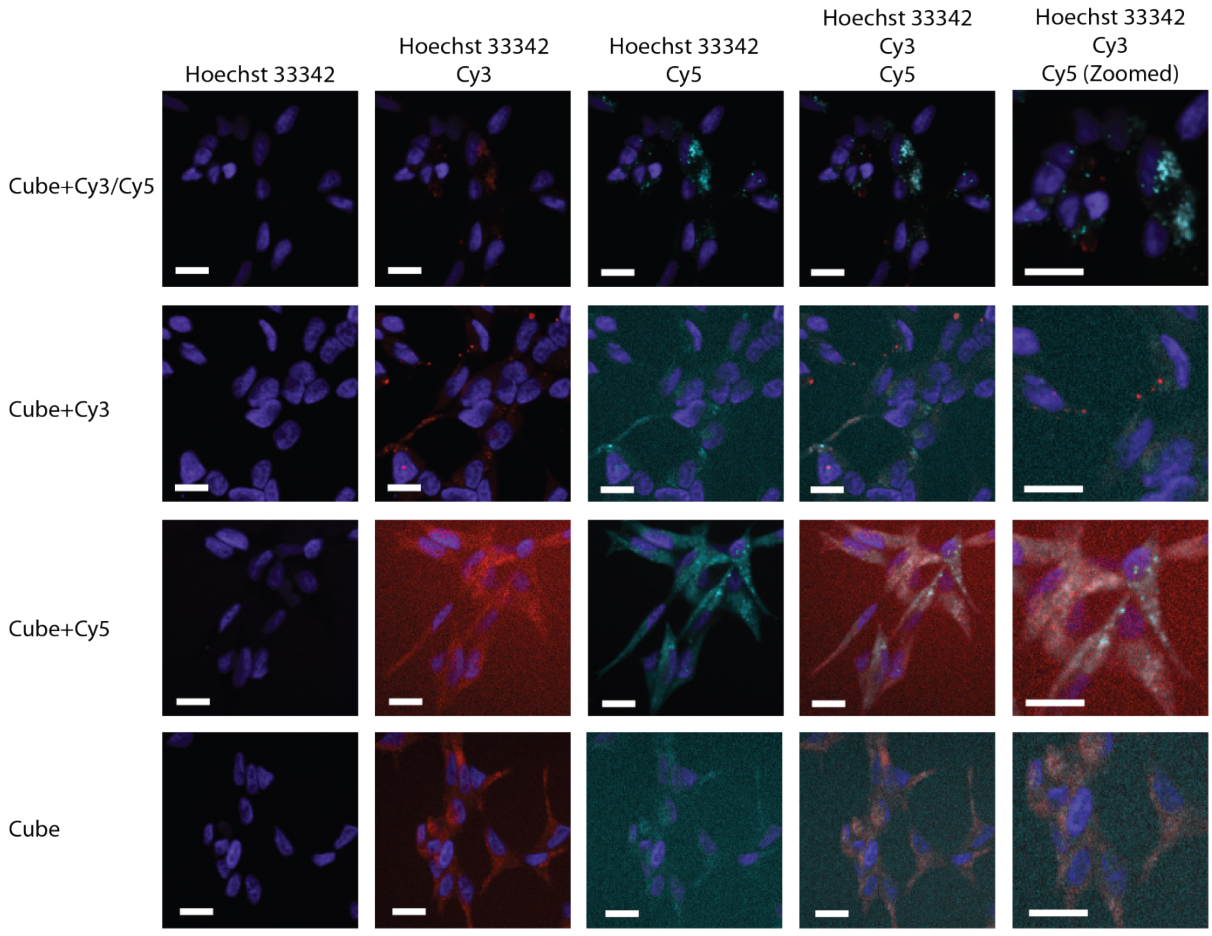

Figure S12: Blunt-ended cube uptake in LNCaP cells. Blunt-ended cubes were incubated unaided with LNCaP cells for 6 hours. Controls include cube labeled with Cy3 only, Cy5 only or no label at all.

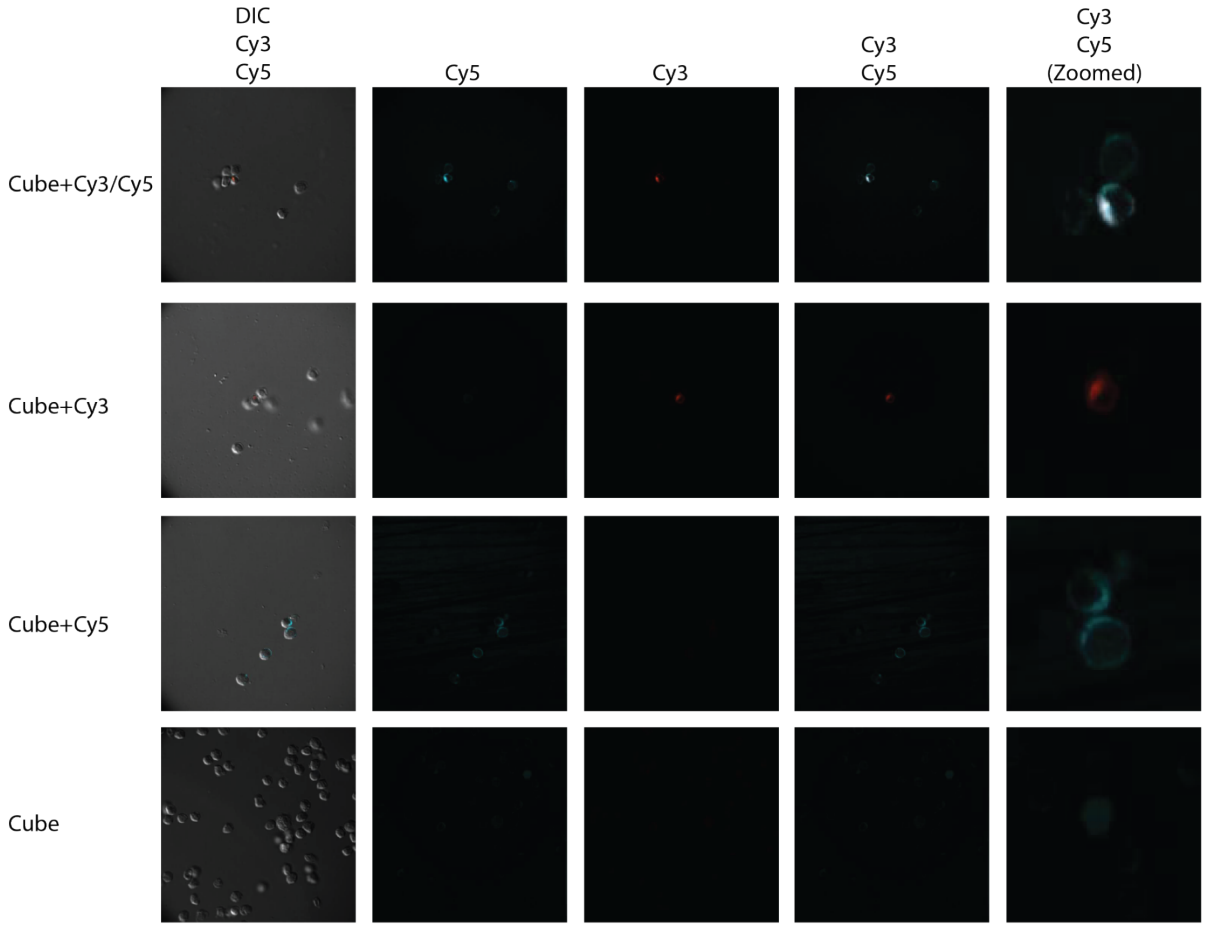

Figure S13: Blunt-ended cube uptake in CLL cells. Blunt-ended cubes were incubated unaided with CLL cells for 6 hours. Controls included singly-labeled cubes with either Cy3 or Cy5 and cubes without labels. These images are a representative example from one patient. CLL cells are suspension cells and non-adherent. They display a different morphology than HeLa and LNCaP cells as a result.

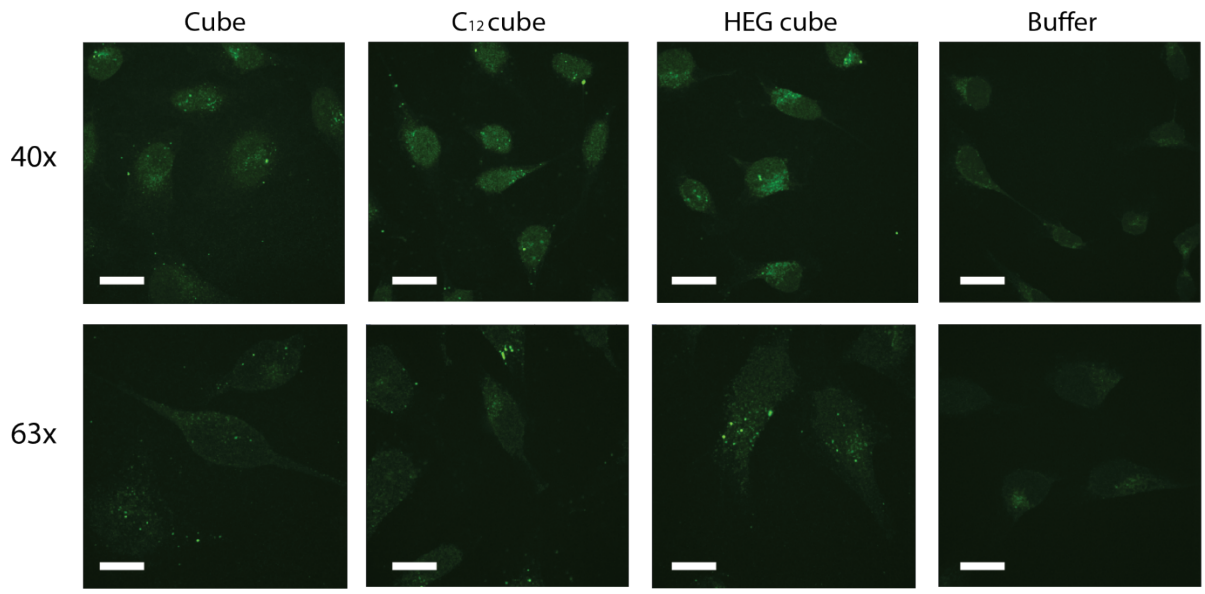

Figure S14: Alexa-488 modified cubes, C_{12} cubes and HEG cubes in HeLa cells. Different cube constructs were incubated with HeLa cells for 24 hours to confirm and compare uptake which is unaided in this case.

c) Fluorescence-activated cell sorting (FACS)

To evaluate the cube uptake using FACS, cells were seeded at a concentration of 50 cells/µl (100 000 cells in 2 ml) in 6-well plates one day prior to the sample incubation. The medium was then replaced in each well with Opti-MEM reduced serum media (1.3 ml) and cube samples were added in triplicates (250 picomoles in 100 µl, 2.5 µM). When mentioned, transfection with oligofectamine was performed by diluting the DNA samples (100 µl) in Opti-MEM (75 µl). To these samples, oligofectamine, (3 µl) diluted in Opti-MEM (12 µl) was added for a final volume of 190 µl. Opti-MEM (90 µl) was added to the other samples to account for the difference in volume. The cells were incubated for 6 hours at 37°C with 5% CO_2. Cells were then washed with PBS (1 ml) and trypsinized. Cells were collected using cold PBS (2 ml) and centrifuged at 1.4 rpm for 5 minutes after which the supernatant was decanted and vacuumed out. The cells were suspended in 200 µl PBS and mixed using a vortex. Paraformaldehyde (4% solution in PBS, 200 µl) was added and the samples were mixed using a vortex. The tubes were sealed and stored at 4°C in the dark until further analysis. It was found that the cube had a robust unaided uptake in HeLa cells. As expected, the uptake was greatly enhanced when

oligofectamine was used as a transfection reagent. Figure S15 summarizes the uptake results in HeLa cells.

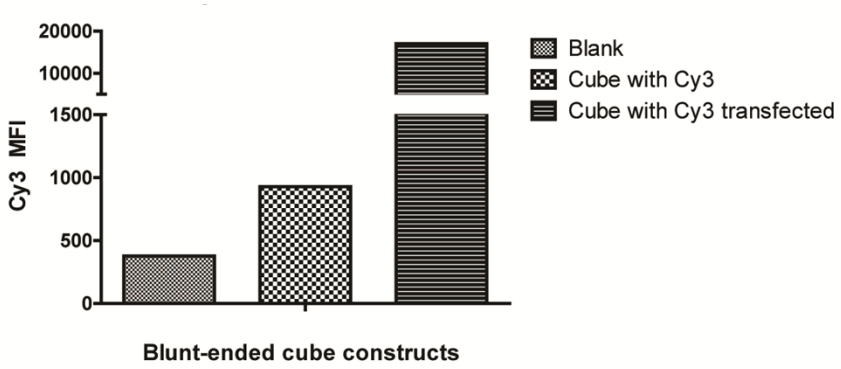

Figure S15: Blunt-ended cube uptake in HeLa cells. Unaided cube uptake was found to be robust by FACS. Oligofectamine transfection increased the cube uptake by a factor of approximately 20.

For the cellular uptake assays involving the cube, the $\mathbf{C_{12}}$ cube and the **HEG** cube, cells were seeded at a concentration of 50 cells/µl (100 000 cells in 2 ml DMEM medium with 10% FBS and antibiotic/antimycotic) in 6-well plates on day before sample incubation. At the start of the assay, the medium was replaced with DMEM without FBS or antibiotic/antimycotic (1 ml) and the samples were added in triplicates (250 picomoles in 200 µl, 1.25 µM). The blank consisted in 200 µl of 1xTAMg buffer and the cubes were assembled using a strand with the same sequence as Unz-5 but with an Alexa-488 dye added on the 3' end. FBS was added up to 10% v/v after 4 hours of incubation at 37°C with 5% CO_2. The cells were then incubated for another 20, 44 or 68 hours depending on the duration of the assay. At the end of the incubation period, cells were washed with PBS (1 ml) and trypsinized. PBS (2 ml) was used to collect the cells and these were then centrifuged at 1.4 rpm for 5 minutes. The supernatant was vacuumed out and the cells were resuspended in 200-400 µl PBS. The cells were then fixed using a 4% paraformaldehyde solution in PBS (200-400 µl). The tubes were sealed and stored in the dark at 4°C until further analysis by FACS. Results demonstrate that the uptake profiles of the cube, the $\mathbf{C_{12}}$ cube and the **HEG** cube vary over time with the $\mathbf{C_{12}}$ cube being favored after shorter incubation times and the **HEG** cube showing increased uptake after longer periods of time.

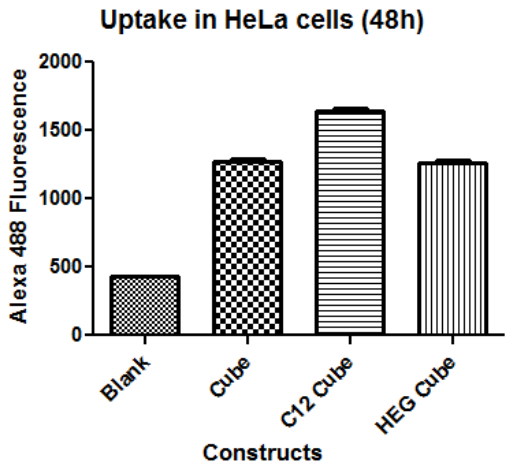

Figure S16: Cube, C_{12} cube and HEG cube unaided uptake in HeLa cells after 48 hours. Three different cube constructs modified with Alexa-488 were incubated in HeLa cells for 48 hours. Results show that the C_{12} cube is favored after this amount of time but this is less striking than after 24 hours suggesting that the other two constructs are taken up more slowly but also more steadily.

X. Image Cross-Correlation Spectroscopy

a) Confocal Microscopy

A confocal laser scanning microscope (CLSM) (Olympus FV300-IX71 (Olympus America)) equipped to collect fluorescence in two detection channels (excitation and filter details in Table S8) was employed to image the Cy3 and Cy5 emission from the cell samples. Images were acquired with a 60x plan-apochromatic NA=1.4 oil objective, with different pixel sizes set by the imaging zoom. Olympus FluoView software was used to collect images in two detection channels, which were then post-processed (averaging and merging), when required, using ImageJ open source software. The CLSM settings were kept constant for every image set (laser power, filters, dichroic mirrors, polarization voltage, and scan speed) so that valid comparisons could be made between measurements from different set of images. Combinations of filters were used to discriminate between the different fluorophores. Table S8 outlines the instrumental settings used for confocal microscopy.

Table S8: LSM Settings for Confocal Microscopy

Targeted fluorophore (s)	Laser	Filters (nm)	Photomultiplier Tube Voltage (V)
GFP, Fluorescein	M_Ar2 (488 nm)	510LP	650
Cy3	HeNe-G (543 nm)	510LP, 605LP	650
Cy5	HeNe-R (633 nm)	660LP	650

b) Cluster Finder (CF) Analysis

An image processing algorithm called cluster finder (CF) was written using Matlab® along with its Image Processing Toolkit (The Mathworks) to analyze the fluorescence images obtained via CLSM. In order to quantify the cellular uptake of the cube, a new program was designed to study the colocalization and correlations of fluorescently-labeled cubes that had been internalized by HeLa cells after a 24-hour incubation period. For these studies, both dually-labeled Cy3-Cy5 cubes, and a 1:1 mixture of singly labeled Cy3/Cy5 cubes, were employed to verify the structural integrity of the cubes and gather information about their uptake patterns. The algorithm CF operates on images obtained from confocal microscopy to yield information such as mean cell intensities, mean number of fluorescent clusters per cell, mean cluster intensities, as well as coefficients pertaining to the colocalization of both clusters and individual fluorophores.

Because the size of the DNA clusters in CLSM images were on the order of the optical point spread function (PSF) (effectively the beam focal spot size), the CF was made to recognize structures with a disc shape with dimensions similar to the PSF. For this reason, a band pass filter was applied to the images to remove all fluctuations that were smaller than the PSF radius (0.3 μm) as well as larger than the expected clusters (diameter > 2 μm). An intensity threshold for each detection channel was also applied to the images. Binary masks were obtained this way for each acquired set of images. Pixels corresponding to cells were also detected using a simple threshold and contiguity algorithm. Only the detected clusters that were in the cell mask were considered. The total intensity of each cluster was computed and the background surrounding each cluster detected was removed. For each image, the total intensity per cell, the number of fluorescent clusters per cell, the intensity per cluster and the center of mass of intensity for each

clusters were computed. To obtain the colocalization of clusters, we defined Cij as being the fraction of clusters i that had their center of mass in the cluster mask of label j. We then obtained C35 and C53, which correspond to the spatial colocalization coefficients of Cy3 and Cy5 clusters. The total intensities of the corresponding colocalized clusters were plotted and were shown to follow a linear relationship as shown by linear regression.

c) CF-ICCS

The CF serves as a powerful tool to identify and characterize clusters within images obtained in one detection channel, but its utility was extended to two detection channels with image cross-correlation spectroscopy (ICCS) to study fluorophore colocalization and intensity correlations[6]. The CF-ICCS program was written in Matlab® and performed two analyses on input images from the two detection channels: intensity cluster correlation studies and spatial ICCS. CF-ICCS first performs the same cluster identification process as CF on individual images from each detection channel; it then superimposes the images and identifies the spatially overlapped clusters.

Single-molecule fluorophore colocalization coefficients (termed M35 and M53) were obtained through spatial ICCS. To measure the colozalization, at the single fluorophore level, ICCS was applied only to the subset of pixels that were in both the Cy3 and Cy5 cluster masks. The procedures are explained in more detail by Balghi *et al.*[7]. The M35 and M53 interaction fractions were obtained as the ratio of the zero spatial lags cross-correlation amplitude to the amplitude of the single channel zero spatial lags autocorrelation amplitude:

$$Mij = \frac{r(0,0)_{ij}}{r(0,0)ii}$$

where r_{ii} is the spatial autocorrelation function of the i channel and r_{ij} is the cross-correlation function of the two channels defined according to spatial lag variables ε and η which represent pixel shifts:

$$r(\varepsilon,\eta)_{ij} = \frac{\langle(\delta I_j(x,y))(\delta I_i(x+\varepsilon,y+\eta))\rangle}{\langle I_i\rangle\langle I_j\rangle}$$

(this equation also defines the single channel spatial autocorrelation function if i = j).

CF-ICCS was used to analyze CLSM images from the following samples: Cy3 and Cy5 dually labeled blunt-ended cubes, a 1:1 mixture of Cy3-labeled blunt-ended cubes and Cy5-labeled blunt-ended cubes as well as a negative control which contained no DNA. CF-ICCS yielded images similar to the example shown in Figure S17, where the image on the left is the overlap of the initial CLSM images for both detection channels and the image on the right is the resulting cluster map calculated by CF.

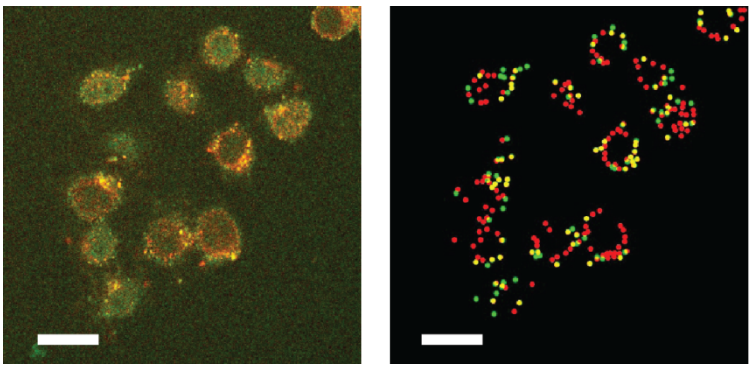

Figure S17: Example of the outputted images from CF-ICCS (enlarged). Green: Cy3. Red: Cy5. Yellow: Overlap of Cy3 and Cy5. Number of pixels: 1024x1024, Magnification: 2X, Pixel size: 0.1150 µm, Cy3 Laser power: 25%, Cy5 Laser power: 25%, Scanning Speed: 9.59sec/image, Averaging: 2

Visual examination of the images shows that the number of red (Cy5) clusters is greater than the number of green (Cy3) clusters, which again suggests that the Cy3 clusters are harder to detect by microscopy than their Cy5 counterparts. The spatial colocalization and ICCS colocalization results are plotted in Figure 3b. For both correlation types, the colocalization coefficient is greater in the sample with the dually-labeled cube (dlDNA) than the sample with the mixture of singly-labeled cubes (slDNA), which is to be expected. However, these results interestingly suggest that there are more Cy5 particles colocalized with Cy3 than vice-versa, but that there are less Cy5 clusters spatially colocalized with Cy3 clusters. This paradox can be explained if the fluophores have different uptake mechanisms.

Intensity cluster correlation studies yielded the following plots which were treated with an averaging bin algorithm to help visualize the correlation and trimmed to only retain the linear region of the plot, which yielded the following linear regressions.

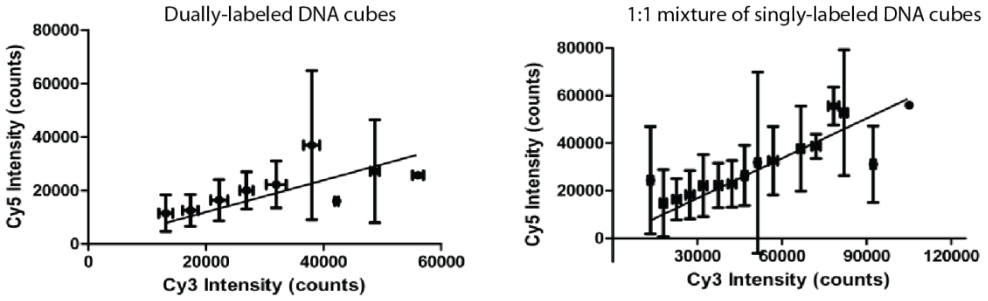

Figure S18. Linear Regressions of the Intensity Cluster Correlation Studies. Bin plots of the fluorescence intensities of Cy3 versus Cy5 in overlapping clusters for dually-labeled cubes (left) and a mixture of singly-labeled cubes (right). The linear regressions yield slopes of 0.60±0.07 and 0.56±0.03, respectively, which are not statistically different, suggesting 1:1 internalization of singly-labeled Cy3 and Cy5 cubes.

Table S9. Linear Regression Statistics

System	m	S_m	b	S_{xx}
dl DNA	0.5963	0.06651	0	7119
sl DNA	0.5606	0.03420	0	8095

The correlation plots slopes are not statistically different for both samples, which suggests that colocalized clusters in both samples have the same relative concentrations of Cy3 and Cy5. Assuming that all Cy3 and Cy5 are identified on the dlDNA, then $c_3 = c_5$ in both samples; this assumption, however, is questionable since the colocalization results do not show 100% colocalization for dlDNA, as it should in theory. It is also noticeable that the range of linearity in intensity counts for dlDNA is [0, 60000], wheres the range of linearity for slDNA is

[0, 120 000], which is twice as large; suggesting that the high-intensity clusters deviate from linearity.

XI. References

1. Beaucage S. L., Iyer R. P., Advances in the synthesis of oligonucleotides by the phosphoramidite approach, Tetrahedron 1992, 48, 12: 2223-2311.
2. Edwardson T. G. W., Carneiro K. M. M., McLaughlin C. K., Serpell C. J., Sleiman H. F., Site-specific positioning of dendritic alkyl chains on DNA cages enables their geometry-dependent self-assembly, Nature Chemistry 2013, 5, 868-875.
3. Conway J. W., McLaughlin C. K., Castor K. J., Sleiman H. F., DNA nanostructure serum stability: greater than the sum of its parts, Chem. Comm. 2013, 49, 1172-1174.
4. Amrein L., Loignon M., Goulet A. C., Dunn M., Jean-Claude B., Aloyz R., Panasci L., Chlorambucil cytotoxicity in malignant B lymphocytes is synergistically increased by 2-(morpholin-4-yl)-benzo[h]chomen-4-one (NU7026)-mediated inhibition of DNA double-strand break repair via inhibition of DNA-dependent protein kinase, J. Pharmacol. Exp. Ther. 2007, 321: 848-55.
5. Panasci et al., Transport, Metabolism, and DNA Interaction of Melphalan in Lymphocytes from Patients with Chronic Lymphocytic Leukemia, Cancer Res. 1988, Apr. 1, 48 (7): 1972-6.
6. Comeau J. W. D., Costantino S., Wiseman P. W., A guide to accurate fluorescence microscopy colocalization measurements, Biophys. J. 2006, 91: 4611-4622.
7. Balghi H., Robert R., Rappaz B., Zhang X., Wohlhuter-Haddad A., Evagelidis A., Luo Y., Goepp J., Ferraro P., Roméo P., Trebak M., Wiseman P. W., Thomas D. Y., Hanrahan J. W., Enhanced Ca^{2+} entry due to Orail plasma membrane insertion increases IL-8 secretion by cystic fibrosis airways, FASEB J. 2011, 12:4274-91.